Advances in Computational Design, *Vol. 9, No. 4 (2024) 285-306*
https://doi.org/10.12989/acd.2024.9.4.285

Comfort level investigation of chromite composite floor system under human walking load

Farhad Abbas Gandomkar*[1] and Wan Hamidon Wan Badaruzzaman[2a]

[1]Department of Structure, Faculty of Civil Engineering, Jundi-Shapur University of Technology, Dezful, Iran
[2]Chairman of Smart and Sustainable Twonship Research Centre (SUTRA), Faculty of Engineering and Built Environment, Universiti Kebangsaan Malaysia, 43600 Bangi, Selangor Darul Ehsan, Malaysia

(*Received February 16, 2019, Revised October 31, 2024, Accepted November 1, 2024*)

Abstract. The main objective of this paper is determining comfortableness of a composite structural floor system known as Chromite. For this purpose, twenty eight Chromite panels were developed via Finite Element Method (FEM) to find their Fundamental Natural Frequency (FNF). Then, the studied panels categorized as Low Frequency Floor (LFF) or High Frequency Floor (HFF) regarding to their FNFs. Peak accelerations of low and high frequency panels and also static stiffness of high frequency panels were determined and compared with the limit value affirmed by American Institute of Steel and Construction (AISC). Effect of various parameters such as dimension of panel, boundary conditions, rigidity of main beam, adding tie beam, thickness of concrete slab, height of composite joist, space between the joists, rigidity of secondary beam, grade of concrete, damping of panel, and type of path were determined on changing FNF and also peak acceleration and static stiffness of the studied panels, depend to kind of panel as LFF or HFF. The results demonstrated that although some factors decreased and increased peak acceleration and static stiffness of the Chromite system, respectively, the panels could reach high vibration levels resulting in lack of comfortableness for users. In addition, the results show that the Chromite floor system needs to improve to be comfort for users.

Keywords: chromite floor system; comfortableness; human walking load; low and high frequency floor; static and dynamic response

1. Introduction

Human comfort is an important aspect that needs to be considered in the design of structural floor systems. Any local minor damages, weakness of structural or nonstructural components or extreme movements of structures affect the human comfort level (Ellingwood and Tallin 1984 and Ad Hoc Committee on Serviceability Research 1986). Floors of buildings will not be suitable for the human occupancy since users feel uncomfortable. Therefore, the aspect of the human comfort must be carefully addressed in the design of floor buildings. Vibration of structural flooring systems can be a critical criterion affecting the human comfort and this is normally generated by human activities

*Corresponding author, Assistant Professor, Ph.D., E-mail: Farhad@jsu.ac.ir
[a] Ph.D., E-mail: wanhamidon@ukm.edu.my

https://techno-press.org/?journal=acd&subpage=5 ISSN: 2383-8477 (Print), 2466-0523 (Online)

(in residential buildings, offices, hotels and so on) and also by machineries (in industrial buildings) placed on the floor. Alvis (2001) stated that Treadgold was the first person to study vibration of floors under the human walking load in 1828. In 1944, Postlethwaite determined the vibration perception threshold as 'feel'-'no feel' by only 0.03% of g for floor with the FNF lower than 10 Hz, which is much lower than the idea of Mallock at the beginning of the nineteenth century. Mallock presented this threshold by word of 'noticeable' with 1% of g. However, the exact meaning of noticeable was not explained. In addition, Dieckmann in 1958 experimentally determined the vibration perception threshold as 0.4% of g. Furthermore, Pretlove and Rainer respectively in 1991 and 1995 compiled data from different sources and proposed a vibration perception threshold for peak acceleration as 0.34% g and they referred to it as "just perceptible". Eriksson in 1994 carried out a similar exercise by compiling all available data based on RMS accelerations for offices and deduced that acceptable RMS acceleration levels are 0.02-0.06 m/s^2 (0.2-0.6% g), depending on the type of offices labelled as "special", "general" or "busy" (Pavic and Reynolds 2002). In addition, according to Gandomkar (2012) various codes presented criterion to define comfortableness of floors for various applications such as schools, residential houses, and offices when human walking load applied on them. The mentioned codes are such as: Appendix G of the Canadian Standards Association Standard CSAS16.1 (CSA), Steel Construction Institute (SCI-P354), NRCC 28482, BS 6472, American Society of Civil Engineers (ASCE 7-05) in its Appendix C, the National Research Council Canada 32349 (NRCC) (Allen and Rainer 1976, Allen *et al*. 1987, SCI 2007, BS 6472 1992, ASCE/SEI 7-05 2006, NRCC 32349 1990). Furthermore, the International Standards Organization (ISO 2631-2 1989) recommended limits as a baseline in terms of RMS acceleration and multiples of base line curve in terms of peak acceleration to make floors comfortable under human activities, as illustrated in Fig. 1. As it is shown in Fig. 1, the peak acceleration limits is obtained by multiplying the baseline with 10 for offices and residences, 30 for indoor footbridges, shopping malls, as well as floors used in dining and dancing, and 100 for outdoor footbridges and floors used in rhythmic activities. American Institute of Steel Construction (AISC 1997) in 11th Steel Design Guide Series, proposed the recommendation of ISO 2631-2 (1989) for floors and stated that the reaction of people who feel vibration depends on their activities. People in offices or residences, and those who take part can respectively accept peak accelerations of about 0.5 and 5 percent of the acceleration of gravity (g). Moreover, people dinning beside a dance floor, lifting weight beside an aerobics gym, or standing in a shopping mall may accept peak acceleration equal to 1.5 percent of g. Allen and Murray in 1993 presented the same suggestion likeness the AISC; a limit state of ISO 2631-2 for offices and commercial buildings when user walk across the floor.

Several studies have been carried out on the dynamic analysis of various structural floor systems. The results of these studies were compared with limiting criteria of codes, standards, and guidelines in order to uncover their comfortableness. Sandun de Silva and Thambiratnam, da Silve *et al*. El-Dardiry and Ji, Williams and Waldron, Chen determined dynamic responses of composite floors under human activities to assess their vibration serviceability (De Silva and Thambiratnam 2009, da Silva *et al*. 2003, 2006, El-Dardiry 2005, Williams 1994, Chen 1999). Ellingwood and Tallin (1984) mathematically studied the dynamic response of floors under a pragmatic model instead of the pedestrian dynamic load. Experimental serviceability criteria were also reported to minimize the vibration of the floors. Smith and Chui (1988) presented a usable method for designers based on a flow chart to evaluate the dynamic response of lightweight wood-joist floor by determination of natural frequency and RMS acceleration of the system under the heel-drop impact load. Howard and Hansen (2003) studied the vibration analysis of waffle floors based on a mathematical method for several manufacturing buildings which was also verified by finite element and experimental results. Foschi *et al*. (1995) carried out an experimental and analytical study on the vibration response of wood floors as a lightweight panel, useful in residential and commercial buildings, under impact load induced by users. Occupants were modeled by two simple oscillators, one degree of freedom and two degrees of freedom. Osborne and Ellis (1990) presented a study on a long-span lightweight floor system with FNF lower than 10 Hz, by the analysis of various methods to evaluate the vibration acceptability of the system through obtaining FNF, damping ratio and acceleration. Willford *et al*. (2007) reviewed five methods to predict the response of structures under the footfall load. The study was performed in two parts; floor and bridge with the FNF lower and greater than 10 Hz. Mello *et al*. (2008) also studied dynamic analysis of a composite system made of concrete slab and steel beams. The research was conducted on acceptability of studied models under four types of dynamic loads which were represented by human walking load by measurement of peak accelerations of panels and comparison with limit of codes. The dynamic response of the mentioned floors was investigated by using FEM as a modern computational tool for structural analysis. Gandomkar *et al*. (2012) determined dynamic response of a composite floor system known as Profiled Steel Sheet Dry Board (PSSDB) with Concrete infill (PSSDBC) to evaluate its comfortableness under human walking load. Also, Gandomkar *et al*. (2013) revealed dynamic response of the PSSDB composite floor system to evaluate its comfortableness when human walking load applied on it. In both studies, the peak accelerations of the studied panels were determined and compared with the limiting value proposed by the standard code of ISO 2631-2 (1989). Effects of changing various parameters on the dynamic responses of the PSSDB and PSSDBC panels were assessed. The results showed that the low frequency PSSDB and PSSDBC panels were not comfort for users. Costa-Neves *et al*. (2014) determined natural frequencies and modes vibration of a composite steel-deck floor system in a multi-story multi-bay building. They utilized the natural frequencies of the system to evaluate its comfortableness. They evaluated acceleration of a steel-composite floor system to predict its comfortableness. For this purpose, they estimated natural frequencies and mode shapes of the studied panels with real spanning of 40m by 40m. Jarnero *et al*. (2015) determined natural frequencies, damping ratios, and mode shapes of a prefabricated timber floor system, experimentally. They found results under various boundary conditions and different stages of construction. Devin *et al*. (2015) revealed effect of non-structural partitions on modal properties of a concrete slab floor system. They compared the natural frequencies of the proposed floor with partitions and the bare floor. They found that partition can increase FNF of the floor system by 30%. These results use directly in analysis of floors in the case of comfort evaluation. An *et al*. (2016) presented dynamic performance characteristics of and innovative composite floor system known as CSBS-CSCFS, under human-induced load. They found experimentally that vibration of the mentioned floor is affected by some parameters such as: dynamic characteristics of the floor, type of human-induced load, stationary people occupying the floor, synchronism of activities, crowd size and load frequency. They compared the results of dynamic responses of the floor with ISO and AISC criteria, to present comfortableness of the studied floor system. Gaspar *et al*. (2016) investigated dynamic behavior of building steel-concrete composite floor system when the floor submitted to human rhythmic activities. The structural model was a real building steel-concrete composite floor system. They found the mentioned type of structural floor system can reach high vibration levels that can compromise the user's comfort. They also simulated a multiple tune mass damper to provide the human comfort. Carmona *et al*. (2017) used a tuned mass damper with friction damping to control excessive floor vibrations. They performed experimental tests by doing rhythmic activities of continuous jumping, walking randomly and synchronized movements with semi bended knees. The results affirmed that the tuned mass damper can reduce response

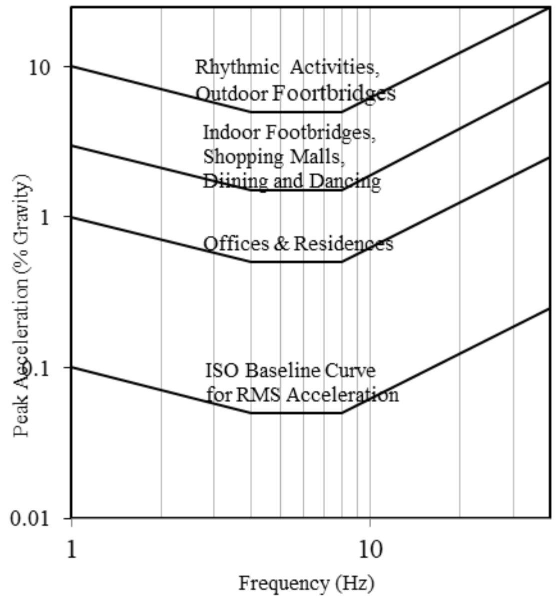

Fig. 1 Recommended peak acceleration for human comfort for vibrations due to human activities (ISO 2631-2 1989)

acceleration of the studied floor system. Friehe *et al*. (2017) presented an assessment method to design of floors with highly vibration sensitive equipment. To achieve their aim, they considered different walking loads. The results visualized graphically to predict the floor vibration due to human load. Mohammed *et al*. (2018) presented an improved model for human induced vibrations of high-frequency floors. They found that improved model shifts the suggested cut-off frequency between low and high frequency floors from 10 Hz to 14 Hz. In addition, the results show that while the existing model presents overestimate or underestimate the vibration levels depending on the pacing rate, the new model offers statistically reliable estimations of the vibration responses. Therefore, it can be adopted in a new generation of the design guidelines featuring a probabilistic approach to vibration serviceability assessment of high-frequency floors.

In accordance with Middleton and Brownjohn (2010), there is little energy in the higher harmonics after four harmonics of a walking force (approximately 10 Hz). A floor is HFF, if it has a FNF above 10 Hz. But, it is known as a LFF if it is dominated by resonance from the first four harmonics of a walking force. Ljunggren *et al*. (2007) stated that some researchers suggested two different design criteria for floor; deflection criteria for HFF and an acceleration limit for LFF. However, the AISC (1997) recommended acceleration limit for LFF and HFF and a minimum static stiffness of 1 kN/mm under concentrated load as an additional check for HFF.

This paper deals with the response of low and high frequency Chromite floor system (Fig. 2), used as offices and residences, under human walking load to determine its comfortableness. Twenty-eight Chromite panels were studied to reveal effect of various parameters such as: dimension of panel, boundary conditions, rigidity of main and secondary beam, adding tie beam, thickness of concrete slab, height of composite joist, space between the joists, grade of concrete, damping of floor panel, and type of path, on changing FNF and also static and dynamic response of low and high frequency Chromite floor system. To achieve the main objective of this study, firstly natural

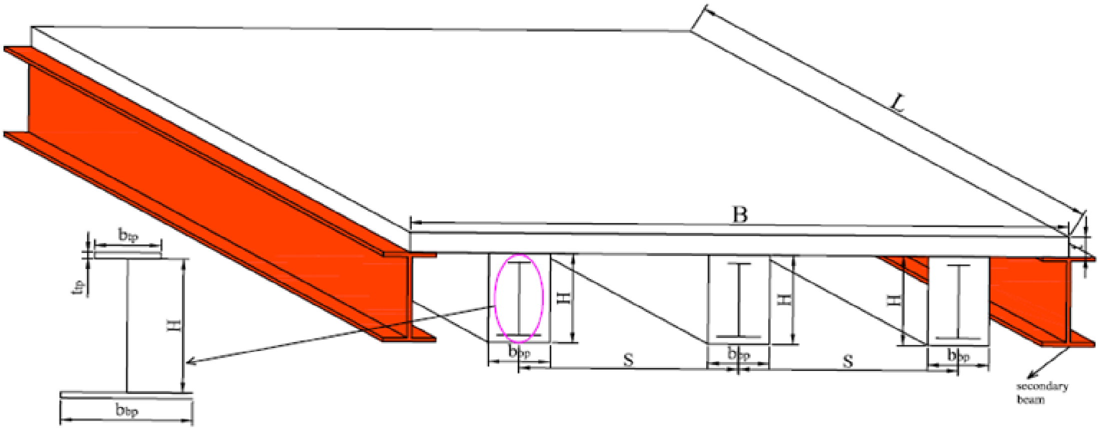

Fig. 2 Chromite floor system

frequencies and vibration modes of all studied panels were obtained. Secondly, regarding to suggestion of the AISC, peak acceleration of studied LFFs and also static stiffness and peak acceleration of studied HFFs were determined and compared with limiting values, affirmed by the AISC (1997).

2. Human-induced dynamic loads

Vibration of floors under human rhythmic activities is a very complex problem with respect to mathematical or physical characterization of this phenomenon because the properties of dynamic vibration of these activities are interconnected to the individual body adversities and the ways which human performs a certain rhythmic activity (Mello *et al*. 2008). A number of studies tried to introduce dynamic loads representing human activities. These studies are summarized in the study of Gandomkar (2012) and Gandomkar *et al*. (2011, 2012).

In the current study, dynamic responses of the studied panels were determined under following four dynamic human walking loads to evaluate their vibration acceptability (Gandomkar *et al*. 2011, 2012).

2.1 First load model

First load model which represents people walking is shown by Gandomkar *et al*. (2011, 2012).

$$F(t) = P\alpha_i \cos(2\pi i f_s t) \tag{1}$$

where:

P: individual's weight, taken as 700-800 N;
α_i: dynamic coefficient for the ith harmonic force component;
i: harmonic multiple of the step frequency;
f_s: step frequency;
t: time in seconds.

Table 1 Loading frequencies, dynamic coefficients, and harmonic phase angles (Mello *et al*. 2008)

Harmonic i	Person walking			
	if_s (Hz)	α_i	Φ	
			Second and third load model	Fourth load model
1	1.6-2.2	0.5	0	0
2	3.2-4.4	0.2	$\pi/2$	$\pi/2$
3	4.8-6.6	0.1	$\pi/2$	π
4	6.4-8.8	0.05	$\pi/2$	$3\pi/2$

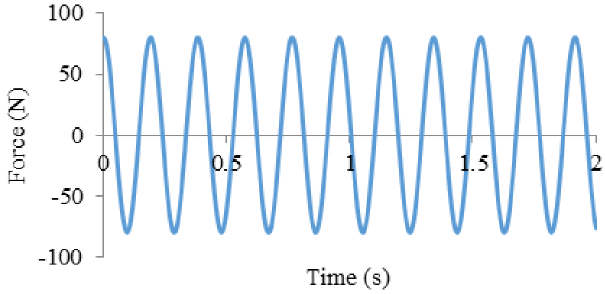

Fig. 3 First load model for PN1

In the first load model, only one resonant harmonic of the load was considered. The harmonic multiple of the step frequency was adopted from Table 1 which depends on the FNF of the panel. For example, if calculated FNF of a panel is equal to 5.2271 Hz (Panel Number (PN) of 1 = PN1), according to Table 1, only third harmonic of the walking loads with step frequency of f_s =1.74 Hz (3 × 1.74 Hz = 5.2271 Hz) should be used in Eq. (1) to determine the first applied load on the panel. Fig. 3 illustrates the first dynamic load model for the panel with FNF of equal to 5.2271 Hz.

2.2 Second load model

The second load model that represents human walking load is presented as below (Gandomkar *et al*. 2011, 2012).

$$F(t) = P\left[1 + \sum \alpha_i \cos(2\pi i f_s t + \Phi_i)\right] \tag{2}$$

where:

P: person' weight;

α_i: dynamic coefficient for the harmonic force;

i: harmonic multiple ($i = 1.2.3. \ldots .n$);

f_s: activity step frequency (dancing, jumping, aerobics or walking);

t: time;

Φ_i: harmonic phase angle

Unlike the previous load model, this load was composed of a static parcel and a combination of four time-dependent repeated loads presented by Fourier series. Four harmonics (see Table 1) were adopted to produce the dynamic second load model. Considering a panel the same as the discussed

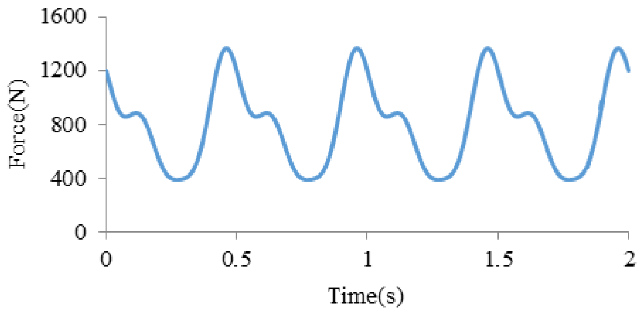

Fig. 4 Second and third load models for PN1

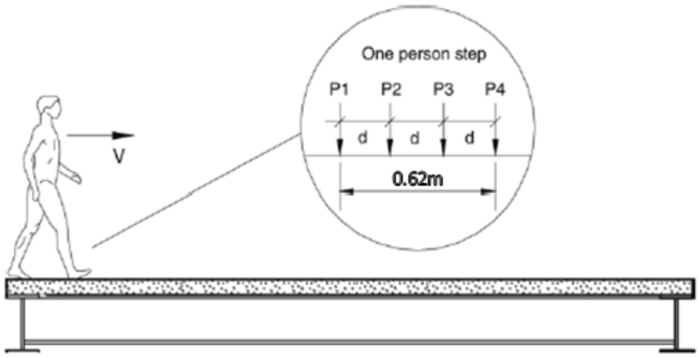

Fig. 5 Person walking on the Chromite floor panel

panel in the previous load model with the FNF equal to 5.2271 Hz, the third harmonic with a step frequency of 1.74 Hz (3 × 1.74 Hz = 5.2271 Hz) was the walking load resonant harmonic. Table 1 shows the dynamic coefficients and phase angles for each harmonic which were used to produce second dynamic load model, as depicted in Fig. 4.

2.3 Third load model

The mathematical function of the third load model which represents the human walking load is similar to the second one, presented in Eq. (2). Similar to the previous load model, the third harmonic with a step frequency of 1.74 Hz was is the resonant harmonic of human walking load (see Table 1). The third load model is more pragmatic than the last two kinds of the load models, as the position of this load changes across the singular location of the floor system (see Fig. 5).

In this kind of load, study of some other parameters related to the step frequency such as step distance and speed of walking, presented in Table 2, is necessary. Also, finite element mesh should be very fine in the third dynamic load model. The contact time of application of the dynamic load with floor was calculated from the step distance and step frequency (see Table 2). In this load model, the subsequent scheme was followed: In a panel identical to the panel in the previous load models, and according to Table 1, the step frequency was equal to 1.74 Hz when the third harmonic was as the resonant harmonic. Therefore, according to Table 2, the step distance was equal to 0.62 m (see Fig. 5).

Table 2 Person walking characteristics (Mello *et al*. 2008)

Activity	Velocity (m/s)	Step distance (m)	Step frequency (Hz)
Slow walking	1.1	0.6	1.7
Normal walking	1.5	0.75	2.0
Fast walking	2.2	1.0	2.3

The step period which corresponds with the step distance of 0.62 m is equal to $1/f = 1/1.74 = 0.57$ s (see Table 2). As it is shown in Fig. 5, four forces were considered representing one human step, which each of the forces as P1, P2, P3, and P4 was applied on the floor during 0.57(contact time)/3 = 0.19 s. The dynamic forces of P1, P2, P3, and P4 were not applied together at the same time. First, the load of P1 was applied on the floor according to Eq. (2) for 0.19s. At the end of this time period, the load of P1 became zero and the load of P2 was applied for 0.19 s. The other loads of the first person step, P3 and P4, were applied in the same procedure described previously. After 0.57 s, the first person step finished and the second person step started and the load of P1 of the second step was equal to the load of P4 in the first step. According to the mentioned method, the process continued repeatedly till all dynamic forces applied along the considered path (see Fig. 12) of the floor.

In this kind of load, study of some other parameters related to the step frequency such as step distance and speed of walking, presented in Table 2, is necessary. Also, finite element mesh should be very fine in the third dynamic load model. The contact time of application of the dynamic load with floor was calculated from the step distance and step frequency (see Table 2). In this load model, the subsequent scheme was followed: In a panel identical to the panel in the previous load models, and according to Table 1, the step frequency was equal to 1.74 Hz when the third harmonic was as the resonant harmonic. Therefore, according to Table 2, the step distance was equal to 0.62 m (see Fig. 5).

The step period which corresponds with the step distance of 0.62 m is equal to $1/f = 1/1.74 = 0.57$ s (see Table 2). As it is shown in Fig. 5, four forces were considered representing one human step, which each of the forces as P1, P2, P3, and P4 was applied on the floor during 0.57(contact time)/3 = 0.19 s. The dynamic forces of P1, P2, P3, and P4 were not applied together at the same time. First, the load of P1 was applied on the floor according to Eq. (2) for 0.19s. At the end of this time period, the load of P1 became zero and the load of P2 was applied for 0.19 s. The other loads of the first person step, P3 and P4, were applied in the same procedure described previously. After 0.57 s, the first person step finished and the second person step started and the load of P1 of the second step was equal to the load of P4 in the first step. According to the mentioned method, the process continued repeatedly till all dynamic forces applied along the considered path (see Fig. 12) of the floor.

2.4 Fourth load model

The fourth dynamic load model representing human walking load is investigated with the same procedure considered in the third one. The principal difference between the third and fourth loads was consideration of the human heel effect in the fourth load which was ignored in the third load model. The human heel effect was uncovered to be an effective parameter on the increase of the load by comparison of the third and fourth load models. According to Mello *et al*. (2008), Varelo in 2004 proposed the mathematical functions of the fourth load model as Eqs. (3)-(6).

$$F(t) = \begin{cases} \left(\dfrac{f_{mi}\,F_m - P}{0.04T_p}\right) t + P \;\; if \quad 0 \le t < 0.04T_p \\ f_{mi}\,F_m \left[\dfrac{C_1\left(t - 0.04T_p\right)}{0.02T_p} + 1\right] \; if \;\; 0.04T_p \le t < 0.06T_p \\ F_m \;\; if \;\; 0.06T_p \le t < 0.15T_p \\ P\left[1 + \sum_{i=1}^{nh} \alpha_i \, sin(2\pi i f_s \left(t + 0.1T_p\right) + \Phi_i)\right] \;\; if \;\; 0.15T_p \le t < 0.90T_p \\ 10(P - C_2) \,.\left(\dfrac{t}{T_P} - 1\right) + P \;\; if \quad 0.90T_p \le t < T_p \end{cases} \tag{3}$$

F_m: maximum Fourier series value, given by Eq. (4);
f_{mi} : heel-impact factor;
T_p: step period;
C_1: coefficients given by Eq. (5);
C_2: coefficients given by Eq. (6).

$$F_m = P\left(1 + \sum_{i=1}^{nh} \alpha_i\right) \tag{4}$$

$$C_1 = (\frac{1}{f_{mi}} - 1) \tag{5}$$

$$C_2 = \begin{cases} P(1 - \alpha_2), & se\; nh = 3 \\ P(1 - \alpha_2 + \alpha_4), & se\; nh = 4 \end{cases} \tag{6}$$

Mello *et al*. (2008) reported that Varela in 2004 and Ohlsson in 1982 declared the impact factor varies person-to-person. In this study, heel-impact factor was adopted equal to 1.12. Fig. 6 shows the dynamic load model of a panel which presented in the previous load models with the FNF of 5.2271 Hz, based on Eqs. (3)-(6).

3. Damping

Damping of structures used in the dynamic analysis is the most difficult item to find. Damping is not an exclusive physical phenomenon in structures dissimilar to mass and stiffness characteristics of a structural system. Therefore, modelling of damping in structures is not accurate like mass and stiffness and its determination is entirely possible based on full-scale measurements (Glanvill *et al*. 1996). In order to obtain damping ratios for floors, applicable design guides and researchers present simple guidance which has been summarized in the study of Gandomkar *et al*. (2011). In addition, the SCI-P354 (2007) are suggested 1.1% damping for completely bare floors or floors where only a small amount of furnishings are present, 3.0% damping for fully fitted out and furnished floors in normal use, and 4.5% damping for a floor where the designer is confident that partitions will be

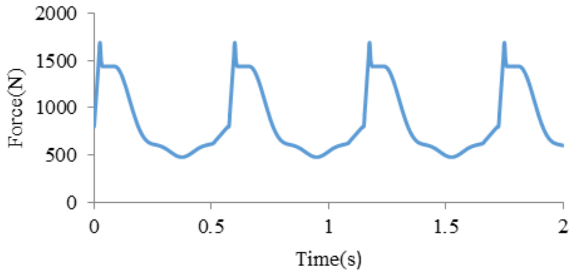

Fig. 6 Fourth load model for PN1

Table 3 Characteristics of Chromite panels

Panel Name	L (mm)	B (mm)	H (mm)	t_{bp} . t_{tp} (mm)	t (mm)	S (mm)	Number of tie beam	Main Beam	Secondary Beam	Number of Secondary Beam	B.Cs
PN1	4000	6000	220	5	50	500	-	240	240	2	B.C.1
PN2	4000	6000	220	5	50	500	-	180	180	2	B.C.1
PN3	4000	6000	220	7	50	500	-	240	240	2	B.C.1
PN4	4000	6000	220	5	100	500	-	240	240	2	B.C.1
PN5	4000	6000	220	5	50	500	-	240	240	2	B.C.2
PN6	4000	6000	220	5	50	500	-	240	240	2	B.C.3
PN7	4000	6000	220	5	50	500	-	240	240	2	B.C.4
PN8	4000	6000	220	5	50	500	-	240	240	2	B.C.5
PN9	4000	6000	220	5	50	500	-	240	240	2	B.C.6
PN10	4000	6000	220	5	50	600	-	240	240	2	B.C.1
PN11	4000	6000	220	5	50	500	-	240	240	5	B.C.1
PN12	4000	6000	220	5	50	500	-	270	270	5	B.C.1
PN13	6000	6000	220	5	50	500	-	240	240	2	B.C.1
PN14	6000	4000	220	5	50	500	-	240	240	3	B.C.1
PN15	6000	4000	220	5	50	500	-	240	240	7	B.C.1
PN16	6000	4000	220	5	50	500	-	240	240	13	B.C.1
PN17	4000	6000	200	5	50	500	-	240	240	2	B.C.1
PN18	8000	6000	220	5	50	500	-	240	240	2	B.C.1
PN19	2000	6000	220	5	50	500	-	240	240	2	B.C.1
PN20	6000	3000	220	5	50	500	-	240	240	2	B.C.1
PN21	6000	7000	220	5	50	500	-	240	240	2	B.C.1
PN22	4000	6000	220	5	50	500	-	140	240	2	B.C.1
PN23	4000	6000	220	5	50	500	1	240	240	2	B.C.1
PN24	4000	6000	220	5	50	500	3	240	240	2	B.C.1
PN25	4000	6000	220	5	50	500	-	240	240	3	B.C.1
PN26	4000	6000	220	5	50	500	-	240	180	2	B.C.1
PN27	4000	6000	220	5	50	500	-	240	140	2	B.C.1
PN28*	4000	6000	220	5	50	500	-	240	240	2	B.C.1

*: All characteristics are same as PN1 but the grade of concrete is C35

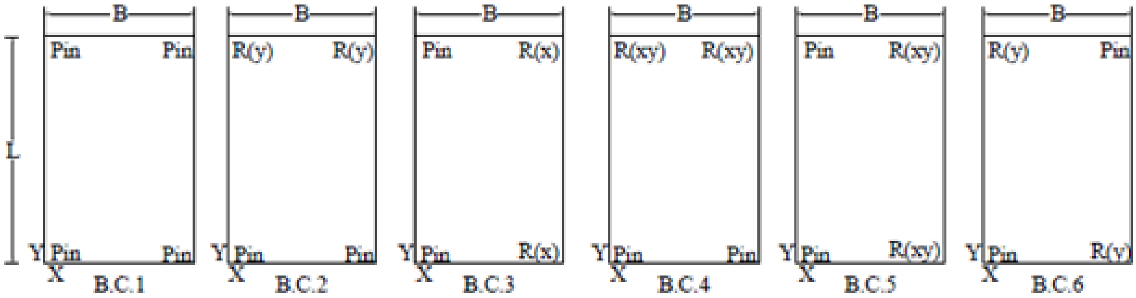

Fig. 7 Boundary conditions of the studied panels

appropriately located to interrupt the relevant mode (s) of vibration (i.e. the partition lines are perpendicular to the main vibrating elements of the critical mode shape). In this study regarding to discussion of Gandomkar *et al*. (2011), the affirmation of the SCI-P354 (1.1%, 3.0%, and 4.5%) are used to introduce in the FEMs.

4. Structural model

The structural model of the system is shown in Fig. 1. The characteristics of the studied panels are presented in Table 3. Boundary conditions (B.Cs) of the studied panels, shown in last column of the Table 3, are illustrated in Fig. 7. The grade of concrete is 30 (C30) in the PN1 till PN27, but this grade is C35 in the PN28.

5. Properties of materials

In this study, dynamic Young's modulus of materials was used as an input of finite element models. According to Murray *et al*. the dynamic Young's modulus for steel can be chosen similar to its static value (BS 5950), i.e., 2.10×10^5MPa (BS 5950 1994). Also, in accordance with BS 8110 (1997), the static Young's modulus of concrete was determined as 24597 MPa for grade 30 concrete. da Silva *et al*. discussed that according to the AISC, in situations where the composite slab is subjected to dynamic excitations, concrete becomes stiffer than the case when it is subjected to pure static loads (da Silva *et al*. 2003, AISC 1997). This issue suggests a 35% increase in the Young's modulus of the conventional concrete (da Silva *et al*. 2003). Therefore, in this study a 33206 MPa dynamic modulus of elasticity was adopted for grade 30 concrete. The Poisson's ratios were adopted as 0.3 for steel and 0.2 for concrete. Also, the density of steel and concrete were chosen 7850 kg/m^3 and 2273 kg/m^3, respectively (Gandomkar *et al*. 2011, 2012).

6. Methodology

To achieve the main aim of the paper, firstly, natural frequencies of the Chromite panels were determined through development of a finite element model by implementation of the ABAQUS program (1992). The developed finite element model was analyzed by "Modal analysis". The

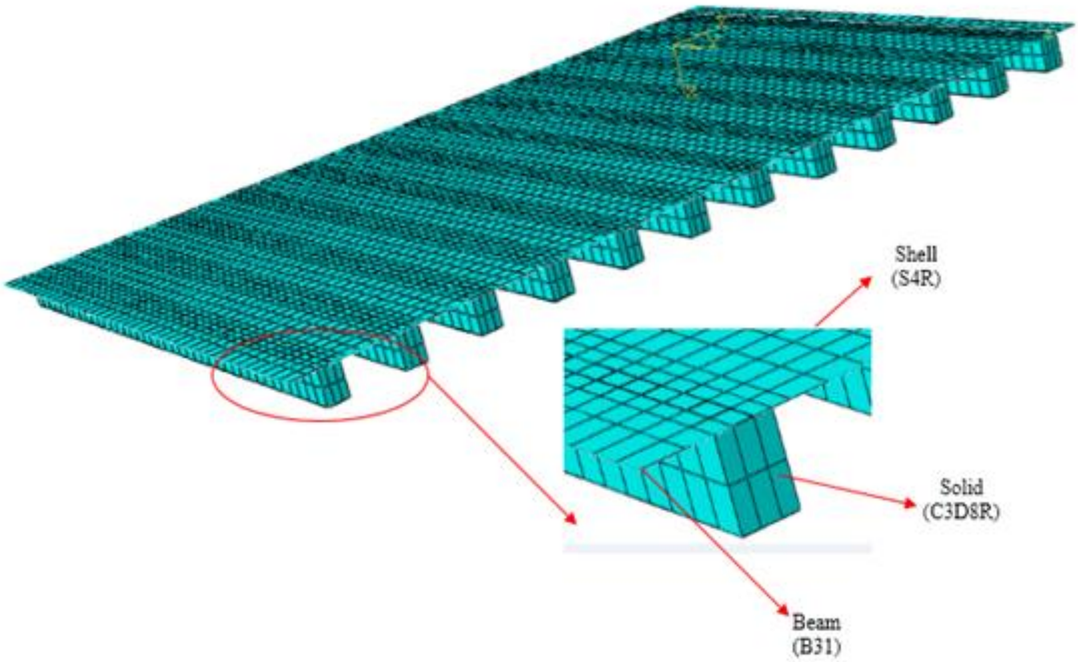

Fig. 8 Computational model of the studied system

“Block Lanczos” method was used to obtain undamped natural frequencies of the studied system. Secondly, regarding to affirmation of the AISC, dynamic analysis was performed on the LFF panels and also dynamic and static analysis were performed on the HFF panels. The results of analysis were peak accelerations for the LFF panels and also peak accelerations and static stiffness for the HFF panels. Determined peak accelerations of the LFF and HFF panels were compared with the affirmation of the AISC (Fig. 1). Also, the AISC, introduced a minimum static stiffness of 1kN/mm under concentrated load as an additional check of the HFF panels. Therefore, static stiffness of the HFF panels were estimated by finite element models and compared with the mentioned criterion of the AISC (1997).

7. Computational model

The FEM presents a more accurate dynamic response especially for structures with involved geometry. Using this method is increased because it can reduce the cost of computing functions (ABAQUS 1992). Therefore, in this study the FEM was used to achieve the aims of the study. Developed finite element models were simulated by the use of fine mesh in the ABAQUS program (1992). In the studied system, the concrete slab and also top and bottom plate of open web steel joist were assigned by S4R shell element. In addition, concrete between composite joists and also tie beams were represented by C3D8R solid element. In the end, the main and secondary beam were modeled by B31 beam element. The finite element model of the PN1 is illustrated in Fig. 8.

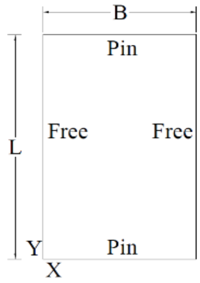

Fig. 9 Boundary condition of verified panel

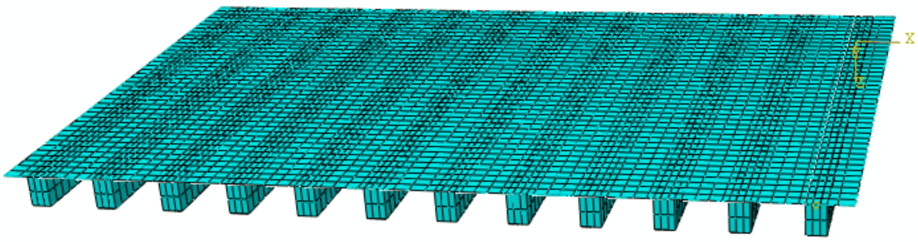

Fig. 10 Finite element mesh of PN1

8. Verification study

As stated, two various analysis were performed to achieve the main objective of this paper; static and dynamic. Therefore, in the case of verification study, first static and dynamic computational models prepared. Then, the results of them compared with the results of affirmation of the AISC (1997). For this purpose, the PN1 has been selected to define accuracy of the results of finite element models. Both static and dynamic verification studies are presented in the following.

8.1 Static verification study

The boundary conditions and finite element model of the PN1 is illustrated in Fig. 9 and Fig. 10. The finite element model of the panel was prepared based on the material properties and type of elements which mentioned before.

According to the AISC, a 1 kN concentrated load applied on the center of the panel (AISC 1997). Static analysis was performed on the simulation and deflection of the center was determined by 0.03736 mm. According to the AISC, a floor with the boundary conditions at the two ends of floor (same as shown in Fig. 9) can be represented by a beam. The AISC proclaims a formula to calculate deflection of mid-span of a beam as Eq. (7).

$$\Delta = \Delta_j + \Delta_g = \frac{PL_j^3}{48EI_j} + \frac{PL_g^3}{48EI_g} \tag{7}$$

where

Δ_j and Δ_g: maximum deflection of the beam or joist and girder, respectively

P: Constant force equal to 1 kN

L_j: the length of floor
L_j: the width of floor
I_j: Moment of inertia along the length
L_j: Moment of inertia along the width
E: module of elasticity
The Eq. (7) has been used to calculate deflection of the center of PN1 which determined by 0.03600 mm. Comparing between the results of FEM and mathematic formula is shown a difference by 3.5%. Therefore, the error of finite element model is acceptable and so the model can present static results with the good accuracy.

8.2 Dynamic verification study

In the case of verification study for the dynamic analysis of the studied system, FNF of the PN1 which determined by FEM was compared with FNF of the mentioned panel which calculated by mathematic fundamental formula, presented by the AISC This formula (Eq. (8)) is used to calculate FNF of a simply supported steel framed floor system (AISC 1997).

$$f = \frac{\pi}{2}\sqrt{\frac{gEI}{WL^4}} \tag{8}$$

where
f: FNF (Hz)
g: acceleration of gravity ($9.806 m/s^2$)
E: modulus of elasticity of steel
I: transformed moment of inertia
W: uniformly distributed weight per unit length (actual, not design, live and dead loads) supported by the member
L: member span
As a result, FNF of the PN1 was determined by 36.384 Hz and 36.44 Hz from finite element model and Eq. (8) respectively. Therefore, error of the FEM was calculated by 0.15%. The mentioned error shows that the developed finite element model can predict the FNF of the system with the high accuracy. On the other hand, first four vibration modes of the PN1 are shown in Fig. 11. The first mode of vibration is bending mode which show the correct behavior of the studied panel.

9. Results and discussion

9.1 FNFs of the studied panels

The studied panels should be categorized as LFF or HFF based on their FNFs to determine type of their analysis. In addition, the FNFs of the panels are used for their dynamic analysis. The FNFs of the studied panels and their categorization are presented in Table 4. In this Table, the PN1 is considered as the base panel, which the FNFs of other panels are compared with its FNF.

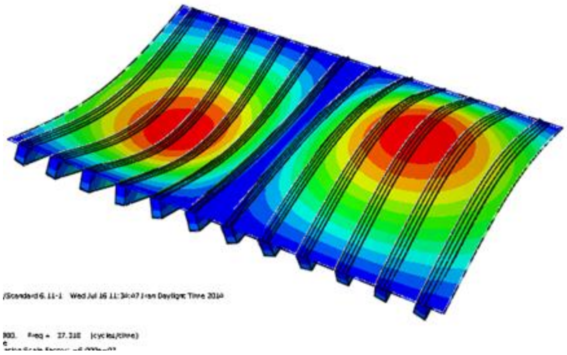

(a) Mode shape associated to the first natural frequency: f_{02}= 37.318 Hz

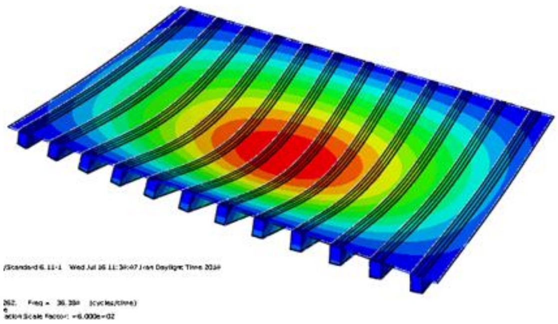

(b) Mode shape associated to the second natural frequency: f_{01}= 36.384 Hz

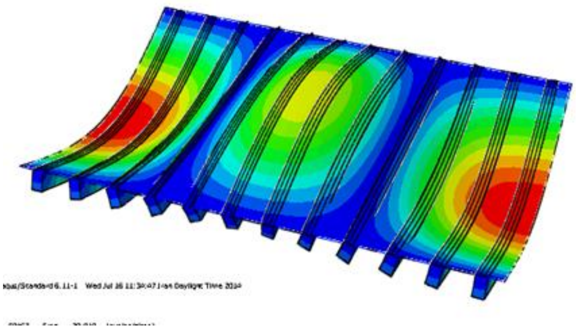

(c) Mode shape associated to the third natural frequency: f_{03}= 38.810 Hz

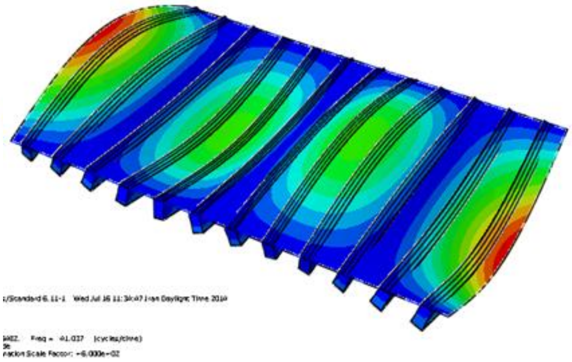

(d) Mode shape associated to the fourth natural frequency: f_{04}= 41.037 Hz

Fig. 11 Floor vibration modes of PN1

Table 4 FNF and categorization of studied panels

Panel Number	FNF (Hz)	Category	PD (%)	Panel Number	FNF (Hz)	Category	PD (%)
PN1	5.2271	LFF	0	PN15	10.255	HFF	96.2
PN2	3.3802	LFF	-35.3	PN16	11.146	HFF	113.2
PN3	5.1772	LFF	-0.95	PN17	5.3367	LFF	2.1
PN4	5.5882	LFF	6.9	PN18	3.6673	LFF	-29.8
PN5	6.4604	LFF	23.6	PN19	7.1159	LFF	36.1
PN6	5.2278	LFF	0.01	PN20	12.191	HFF	133.2
PN7	6.4606	LFF	23.6	PN21	6.4706	LFF	23.8
PN8	7.8817	LFF	50.9	PN22	2.4961	LFF	-52.2
PN9	7.9935	LFF	52.9	PN23	6.5285	LFF	24.9
PN10	5.4774	LFF	4.8	PN24	7.9773	LFF	52.6
PN11	7.4542	LFF	42.6	PN25	6.1654	LFF	17.9
PN12	8.6522	LFF	65.5	PN26	5.2263	LFF	-0.015
PN13	4.3056	LFF	-17.6	PN27	5.2259	LFF	-0.023
PN14	9.4072	LFF	80	PN28	5.2486	LFF	0.41

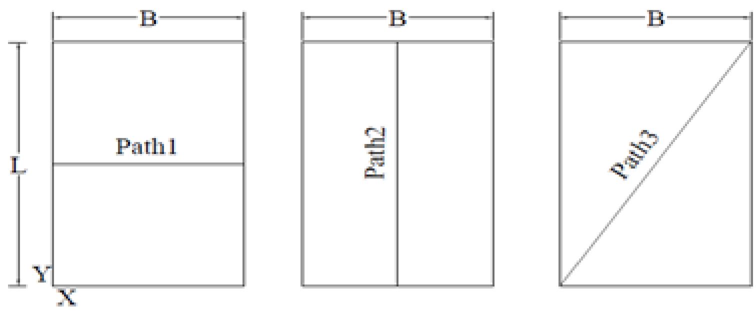

Fig. 12 Layout of paths

The results show that changing in dimensions of the system, its boundary conditions, rigidity of main beam, and also adding tie beam, significant changes the FNF of the system up to 133.2%, 52.9%, -52.2%, %52.6%, respectively. In addition, increasing thickness of concrete slab and distance between composite joists increases the FNF of the system up to 6.9% and 4.8%, respectively. Furthermore, the results demonstrate that variation in rigidity of secondary beam, height of composite joist, and thickness of top and bottom flanges of open web steel joists, insignificant changes the FNF of the studied system up to -0.023%, 2.1%, and -0.95%, respectively. Finally, the results uncover that changing in grade of concrete changes the FNF of the system only by 0.41%.

9.2 Static and dynamic responses of the studied panels

Based on the FNFs of the studied panels, the category of the panels (LFF or HFF) were revealed. Then, regarding to the main goal of the study, dynamic analysis was performed to determine peak acceleration of LFFs and also static and dynamic analysis were performed to determine static stiffness and peak acceleration of HFFs, respectively. Four dynamic load models applied on the studied panels representing human walking load which described previously. Three paths were considered as illustrated in Fig. 11. The paths show direction of people who move on the floor. Three damping ratios (1.1%, 3%, and 4.5%) were considered regarding to affirmation of the SCI-P354 (2007).

The results of the analysis of the studied panels are presented in Table 5. The obtained accelerations of LFFs and HFFs were compared with the proposed peak acceleration limit by the ISO 2631-2, affirmed by the AISC (1997). Also obtained static stiffness of the HFFs were compared with the proposed minimum static stiffness limit by the AISC (1 kN/mm under concentrated load at the center of panel).

Table 5 presents a lot of information about effect of various parameters on the static and dynamic response of the studied system. Therefore, the PN1 is selected to present the base results of the study. According to Table 5, the peak accelerations of the studied panels were evaluated under the second load model which uncovered to be greater than those corresponding evaluated peak accelerations under the first load model. This point revealed that considering four harmonics in the dynamic load is a very important issue in the dynamic responses of the floor and showed a significant effect on the increase of the peak acceleration. As it is obvious from Table 5, when the third and fourth load models were applied on the studied panels, the peak accelerations were higher than those of the applied first and second load models. This fact was highlighted when the position of

Table 5 Peak acceleration and static stiffness of studied panels

Panel Number	ξ%	Peak Accelaretion									Static Stiffness (kN/mm)
		Load I (m/s^2)	Load II (m/s^2)	Load III (m/s^2)			Load IV (m/s^2)			ISO 2631-2	
				Path1	Path2	Path3	Path1	Path2	Path3		
	1.1%	0.169	0.362	0.664	1.266	0.919	1.858	1.166	1.99		
PN1	3%	0.101	0.286	0.376	0.233	0.341	0.690	0.823	0.596	0.4903	-
	4.5%	0.073	0.230	0.266	0.579	0.174	0.368	0.690	0.303		
	1.1%	0.104	0.836	0.568	0.39	-	1.145	1.53	-		
PN2	3%	0.087	0.613	0.119	0.182	-	0.155	0.101	-	0.4903	-
	4.5%	0.074	0.488	0.138	0.032	-	0.153	0.064	-		
	1.1%	0.197	0.437	1.24	0.488	-	1.214	0.790	-		
PN3	3%	0.157	0.266	0.386	0.043	-	0.557	0.087	-	0.4903	-
	4.5%	0.127	0.195	0.458	0.012	-	0.296	0.024	-		
	1.1%	0.138	0.363	0.351	0.114	-	0.902	0.803	-		
PN4	3%	0.087	0.218	0.188	0.029	-	0.362	0.144	-	0.4903	-
	4.5%	0.062	0.159	0.106	0.013	-	0.191	0.043	-		
	1.1%	0.450	0.566	0.685	0.248	-	1.926	1.358	-		
PN5	3%	0.251	0.406	0.681	0.292	-	1.117	0.604	-	0.4903	-
	4.5%	0.178	0.311	0.708	0.144	-	1.092	0.260	-		
	1.1%	0.163	0.340	1.066	0.977	-	1.993	1.36	-		
PN6	3%	0.096	0.340	0.404	0.191	-	0.722	0.265	-	0.4903	-
	4.5%	0.069	0.340	0.219	0.057	-	0.386	0.077	-		
	1.1%	0.449	0.567	0.752	0.253	-	1.915	1.365	-		
PN7	3%	0.251	0.406	0.563	0.292	-	1.077	0.604	-	0.4903	-
	4.5%	0.178	0.311	0.496	0.144	-	0.758	0.260	-		
	1.1%	0.402	0.456	0.170	0.173	-	0.458	0.523	-		
PN8	3%	0.065	0.211	0.017	0.020	-	0.091	0.030	-	0.4903	-
	4.5%	0.065	0.146	0.026	0.002	-	0.056	0.007	-		
	1.1%	0.035	0.271	2.079	0.202	-	2.223	0.486	-		
PN9	3%	0.016	0.203	1.169	0.020	-	1.245	0.040	-	0.4903	-
	4.5%	0.011	0.157	0.915	0.004	-	0.987	0.009	-		
	1.1%	0.1886	0.355	1.516	2.461	-	1.934	1.724	-		
PN10	3%	0.109	0.263	0.403	1.577	-	0.614	1.724	-	0.4903	-
	4.5%	0.078	0.197	0.278	1.345	-	0.354	1.724	-		
	1.1%	0.153	0.4	0.641	0.152	-	0.890	0.449	-		
PN11	3%	0.072	0.076	0.547	0.012	-	0.808	0.040	-	0.4903	-
	4.5%	0.053	0.074	0.689	0.021	-	0.756	0.003	-		
	1.1%	0.241	0.291	0.423	0.467	-	0.726	0.564	-		
PN12	3%	0.146	0.154	0.292	0.034	-	0.292	0.058	-	0.4903	-
	4.5%	0.101	0.114	0.422	0.010	-	0.451	0.025	-		

	1.1%	0.396	0.523	2.664	3.813	-	2.251	4.348	-		
PN13	3%	0.266	0.447	2.057	3.525	-	2.513	3.810	-	0.4903	-
	4.5%	0.204	0.438	2.024	3.534	-	2.478	3.800	-		
	1.1%	0.056	0.330	0.600	0.275	-	0.630	0.367	-		
PN14	3%	0.035	0.161	0.599	0.023	-	0.753	0.042	-	0.4903	-
	4.5%	0.019	0.110	0.725	0.004	-	0.901	0.010	-		
	1.1%	0.018	0.253	0.311	0.264	-	0.565	0.552	-		
PN15	3%	0.010	0.157	0.454	0.060	-	0.732	0.107	-	0.4903	15.768
	4.5%	0.007	0.118	0.598	0.033	-	0.883	0.022	-		
	1.1%	0.032	0.259	0.608	0.362	-	0.444	1.242	-		
PN16	3%	0.020	0.119	0.078	0.448	-	0.131	1.132	-	0.4903	20.938
	4.5%	0.013	0.080	0.025	0.606	-	0.035	1.114	-		
	1.1%	0.256	0.528	0.553	0.162	-	1.318	0.617	-		
PN17	3%	0.192	0.324	0.190	0.009	-	0.454	0.072	-	0.4903	-
	4.5%	0.156	0.237	0.164	0.002	-	0.284	0.026	-		
	1.1%	4.3e-4	4.3e-4	1.940	1.386	-	2.239	1.562	-		
PN18	3%	4e-4	4e-4	1.686	0.510	-	1.960	0.771	-	0.4903	-
	4.5%	3.9e-4	3.9e-4	1.750	0.410	-	1.919	0.833	-		
	1.1%	0.095	0.630	0.825	0.280	-	1.325	0.089	-		
PN19	3%	0.045	0.344	0.393	0.001	-	0.767	0.004	-	0.4903	-
	4.5%	0.032	0.242	0.388	3.2e-4	-	0.718	6.5e-4	-		
	1.1%	6.8e-4	6.8e-4	1.061	0.505	-	1.593	0.505	-		
PN20	3%	6.5e-4	6.5e-4	0.849	0.406	-	1.512	0.410	-	0.4903	8960.5
	4.5%	6.5e-4	6.5e-4	0.838	0.389	-	1.515	0.382	-		
	1.1%	0.133	0.216	0.960	0.905	-	1.337	0.985	-		
PN21	3%	0.048	0.145	1.019	0.301	-	1.439	0.357	-	0.4903	-
	4.5%	0.019	0.113	0.966	0.129	-	1.399	0.156	-		
	1.1%	0.018	0.163	0.123	0.068	-	0.164	0.104	-		
PN22	3%	0.045	0.106	0.129	0.012	-	0.149	0.014	-	0.4903	-
	4.5%	0.061	0.079	0.115	0.003	-	0.12	0.047	-		
	1.1%	0.096	0.193	0.070	0.256	-	0.147	0.417	-		
PN23	3%	0.053	0.156	0.016	0.007	-	0.103	0.011	-	0.4903	-
	4.5%	0.037	0.126	0.012	0.001	-	0.057	0.002	-		
	1.1%	0.079	0.201	0.675	0.245	-	0.743	0.414	-		
PN24	3%	0.038	0.136	0.644	0.014	-	0.707	0.016	-	0.4903	-
	4.5%	0.025	0.102	0.601	0.002	-	0.661	0.003	-		
	1.1%	0.399	0.501	0.641	0.326	-	0.759	0.377	-		
PN25	3%	0.250	0.276	0.488	0.074	-	0.515	0.125	-	0.4903	-
	4.5%	0.198	0.198	0.465	0.029	-	0.481	0.048	-		

PN26	1.1%	0.172	0.361	0.665	1.276	-	1.851	1.156	-	0.4903	-
	3%	0.103	0.288	0.420	0.242	-	0.696	0.835	-		
	4.5%	0.073	0.230	0.383	0.069	-	0.515	0.580	-		
PN27	1.1%	0.173	0.361	0.666	1.15	-	1.85	1.284	-	0.4903	-
	3%	0.104	0.287	0.438	0.241	-	0.692	0.836	-		
	4.5%	0.074	0.230	0.337	0.068	-	0.393	0.581	-		
PN28	1.1%	0.107	0.368	0.675	1.081	-	1.853	1.395	-	0.4903	-
	3%	0.069	0.288	0.324	0.267	-	0.694	0.892	-		
	4.5%	0.053	0.229	0.269	0.074	-	0.386	0.626	-		

the dynamic load changed across the individual direction, the dynamic response of the panels increased. Gandomkar *et al*. (2011, 2012) and Mello *et al*. (2008) also focused on this point and stated that this is a substantial increase in the structure. The peak acceleration of the panels under the fourth load model was assessed higher than those under the third load model. On the other hand, the scheme of loading on the panels in the third and fourth load models was the same as each other. Therefore, this increase should be caused by the heel impact factor ($f_{mi} = 1.12$) used in the fourth load model. In addition, the results demonstrate that increasing of damping ratio has a direct significant effect on decreasing peak acceleration of the system. By comparing the peak acceleration of the PN1 for various considered paths, the results show that the type of path has not distinguish effect on the results.

In accordance with the peak accelerations of the studied panels, when the first and second load models apply on them, some panels are comfort for the users and some of them are not comfort. This situation is depend to characteristics, boundary conditions and damping ratio of the panel (Table 5). In addition, by comparing the peak accelerations of the panels under the third and fourth load models with recommendations of the ISO 2631-2 (1989), it is uncovered that all panels are not comfort for the users.

The results of study with focusing on type of dynamic load model (I, II, III, and IV) demonstrate that changing in the characteristics of the Chromite floor system changes its dynamic response with different phenomena. It means, percent of increase or decrease in peak acceleration of the system under mentioned loads do not have specific rule same as each other. Therefore, effect of applying each different dynamic load model (I, II, III, IV) on the results of study should be investigated independently. For example, by comparing peak acceleration of PN1 (as the base model) with peak acceleration of other panels when the fourth load model (path 2, 3% damping) apply on them, the results show that changing dimension of panel, boundary conditions, rigidity of the main beam, adding tie beam, thickness of concrete slab, rigidity of the secondary beam, height of composite joist, space between the joists, thickness of top and bottom plates of girder, grade of concrete changes peak acceleration of the system up to 6.32%, 26.61%, 98.3%, 98.06%, 82.50%, -1.58%, 91.25%, -109.48%, 89.43%, -8.38%, respectively. Furthermore, by comparing peak acceleration of PN1 with peak accelerations of PN5, PN6, PN7, PN8, and PN9, it is obvious that release sliding in support can decreases the peak acceleration of the system. Also, comparing peak accelerations of the studied panels in various paths (1, 2, and 3) shows different phenomena. So that, prediction of peak acceleration under various types of path is not possible. Moreover, the results show that all high frequency Chromite panels have enough static stiffness.

10. Conclusions

This paper investigates static and dynamic response of low and high frequency Chromite floor system under human walking load to evaluate its comfortableness. Four dynamic load models were used while the third and fourth load models were more pragmatic having two properties; changing load according to the individual position, and generating time function corresponding to the nature of human walking load. The effect of human heel impact was also considered in the fourth load model.

Dynamic responses of the low frequency Chromite panels were obtained in terms of the peak acceleration and compared with the proposed limiting value by the ISO 2631-2 where the panels used as residences and offices. In addition, static and dynamic responses of the high frequency Chromite panels were determined and compared with the limiting value of the ISO 2631-2 (1989) and the AISC (1997). Some of studied panels were shown to be comfortable for users when the first and second dynamic load models applied on them. Also, some of them were not comfort for users. The position of loads was changed across the individual directions when the third and fourth dynamic load models applied on the panels. For these two types of load models, three paths were selected to show the effect of moving direction on the dynamic response of the panels. The peak accelerations of the studied panels under the third and fourth dynamic load models were determined higher than those of the first and second loads and also limiting value of the ISO 2631-2 (1989). Therefore, all panels were not comfort for users when the third and fourth load models applied on them. These results uncovered this fact that changing the position of the load is an effective item in increasing of the response of the panels.

Changing the characteristics of the studied system can change its peak acceleration. In this case, changing dimension of panel, boundary conditions, rigidity of the main beam, adding tie beam, thickness of concrete slab, height of composite joist, and space between the joists changes significant peak acceleration of the system. On the other hand, changing rigidity of the secondary beam and grade of concrete not change peak acceleration of the system, significantly. Enhancement of the damping ratio of the Chromite system can considerably reduce the peak acceleration of the system. These results can be useful to help designers to reduce the response of the Chromite floor by using suitable furniture and type of partitions (2007).

References

Abaqus Analysis User's Manual (1992), Version 6.12.

Ad Hoc Committee on Serviceability Research (1986), "Structural serviceability: A critical appraisal and research needs", *J. Struct. Eng.*, **112**, 2646-2664. https://doi.org/10.1061/(ASCE)0733-9445.

Allen, D.E. and Rainer, J.H. (1976), "Vibration criteria for long span floors", *Canadian J. Civil Eng.*, **3**(2), 165-172. https://doi.org/10.1139/l76-017.

Allen, D.E., Rainer, J.H. and Pernica, G. (1987), *Building Vibration Due to Human Activities (NRCC 28482)*, National Research Council Canada, Institute for Research in Construction, Canada.

Alvis, S.R. (2001), "An experimental and analytical investigation of floor vibrations", M.Sc. Thesis, Virginia Polytechnic Institute and State University, Virginia, U.S.A.

American Institute of Steel Construction (AISC) (1997), *Floor Vibration Due to Human Activity:11th Steel Design Guide Series*, U.S.A.

An, Q., Ren, Q., Yan, X. and Chen, Z. (2016), "Dynamic performance characteristics of an innovative Cable Supported Beam Structure-Concrete slab composite floor system under human-induced loads", *Eng. Struct.*,

117, 40-57. https://doi.org/10.1016/j.engstruct.2016.02.038
ASCE/SEI 7-05 (2006), *Minimum Design Loads for Buildings and Other Structures,* American Society of Civil Engineers, U.S.A.
BS 6472 (1992), *Guide to Evaluation of Human Exposure to Vibration in Buildings (1 Hz to 80 Hz)*, British Standards Institution, U.K.
BS 5950 (1994), *Structural Use of Steelwork in Building: Code of Practice for Design of Composite Slabs with Profiled Steel Sheeting*, Part 4, British Standards Institution, U.K.
BS 8110 (1997), *Code for Practice for Design and Construction. Structural Use of Concrete*, British Standards Institution, Part 1, U.K.
Carmona, J.E.C., Avila, S.M. and Doz, G. (2017), "Proposal of a tuned mass damper with friction damping to control excessive floor vibrations", *Eng. Struct.*, **148**, 81-100. https://doi.org/10.1016/j.engstruct.2017.06.022.
Chen, Y. (1999), "Finite element analysis for walking vibration problems for composite building floor using ADINA: modeling, simulation, and comparison", *Comput. Struct.*, **72**, 109-126. https://doi.org/10.1016/S0045-7949(99)00004-8.
Costa-Neves, L.F., da silva, J.G.S., Lima, L.R.O. and Jordao, S. (2014), "Multi-story, multi-bay building with composite steel deck floors under human-induced loads: the human comfort issue", *Comput. Struct.*, **136**, 34-46. https://doi.org/10.1016/j.compstruc.2014.01.027.
da Silva, J.G.S., da SVellasco, P.C.G., de Andrade, S.A.L., da, F.J., Soeiro, C.P. and Werneck, R.N. (2003), "An evaluation of the dynamical performance of composite slabs", *Comput. Struct.*, **81**, 1905-1913. https://doi.org/10.1016/S0045-7949(03)00210-4.
da Silva, J.G.S., da S Vellasco, P.C.G., de Andrade, S.A.L. and de Lima, L.R.O. (2006), "Dynamic response of composite steel deck floors", *Latin Am. J. Solids Struct.*, **3**, 163-178.
Devin, A., Fanning, P.J., Pavic, A. (2015), "Modelling effect of non-structural partitions on floor modal properties", *Eng. Struct.*, **91**, 58-69. https://doi.org/10.1016/j.engstruct.2015.02.021
The Steel Construction Institute (SCI) (2007), *Design of Floors for Vibration: A New Approach (SCI-P354)*. SCI, U.K.
El-Dardiry, E. and Ji, T. (2005), "Modeling of the dynamic behaviour of profiled composite floors", *Eng. Struct.*, **28**, 567-79. https://doi.org/10.1016/j.engstruct.2005.09.012.
Ellingwood, B., Tallin, A. (1984), "Structural serviceability floor vibrations", *J. Struct. Eng.*, **110**, 401-420. https://doi.org/10.1061/(ASCE)0733-9445(1984)110:2(401)
Foschi, R.O., Neumann, G.A., Yao, F. and Folz, B. (1995), "Floor vibration due to occupants and reliability-based design guidelines", *Canadian J. Civil Eng.*, **22**, 471-479. https://doi.org/10.1139/l95-055.
Friehe M, Heinemeyer, C.H. and Feldmann, M. (2017), "Design of highly sensitive floors for human induced vibrations", *Procedia Eng.*, **199**, 2796-2801. https://doi.org/10.1016/j.proeng.2017.09.549.
Gandomkar, F.A., Wan Badaruzzaman, W.H. and Osman, S.A. (2911), "Dynamic response of low frequency Profiled Steel Sheet Dry Board with Concrete infill (PSSDBC) floor system under human walking load", *Latin Am. J Solids Struct.*, **9**, 21-41. https://doi.org/10.1590/S1679-78252012000100002.
Gandomkar, F.A. (2012), "Determining comfort level of profiled steel sheeting dry board floor system", Ph.D. Dissertation, Department of Civil Engineering, National University of Malaysia, Bangi, Malaysia.
Gandomkar, F.A., Wan Badaruzzaman, W.H. and Osman, S.A. (2012), "Dynamic response of low frequency Profiled Steel Sheet Dry Board (PSSDB) floor system under human walking load", *Latin Am. J Solids Struct.*, **10**, 135-1154. https://doi.org/10.1590/S1679-78252012000100002.
Gasper, C.M.R., Santos, da Silva, G.J., Costa-Neves, L.F. (2016), "Multimde vibration control of building steel-concrete composite floors submitted to human rhythmic activities" *Comput. Struct.*, **165**, 107-122. https://doi.org/10.1016/j.compstruc.2015.12.010.
Glanvill, M.J., Kwok, K.C.S. andDenoon, R.O. (1996), "Full-scale damping measurements of structures in Australia", *J. Wind Eng. Ind. Aerodyn.*, **59**, 349-364. https://doi.org/10.1016/0167-6105(96)00016-5.
Howard, C.Q. and Hansen, C.H. "Vibration analysis of waffle floors", *Comput. Struct.*, **81**, 15-26. https://doi.org/10.1016/S0045-7949(02)00348-6.
ISO 2631-2 (1989), *Evaluation of Human Exposure to Whole-Body Vibration Part 2: Continuous and Shock-*

Induced Vibration in Buildings (1-80 Hz), International Standards Organization, London, U.K.
Jernero, K., Bradt, A. and Olsson, A. (2015), "Vibration properties of a timber floor assessed in laboratory and during construction", *Eng*. *Struct*., **82**, 44-54. https://doi.org/10.1016/j.engstruct.2014.10.019.
Kareem, A. and Gurley, K. (1996), "Damping in structures: its evaluation and treatment of uncertainly", *J. Wind Eng*. *Ind*. *Aerodyn*., **59**, 131-157. https://doi.org/10.1016/0167-6105(96)00004-9.
Ljunggren, F., Wang, J. and Agren, A. (2007), "Human vibration perception from single-and dual-frequency components", *J. Sound Vib*., **300**, 13-24. https://doi.org/10.1016/j.jsv.2006.06.072.
Mello, A.V.A., da Silva, J.G.S., da S Vellasco, P.C.G., de Andrade, S.A.L. and de Lima, L.R.O. (2008), "Dynamic analysis of composite systems made of concrete slabs and steel beams", *J. Constr*. *Steel Res*., **64**, 1142-1151. https://doi.org/10.1016/j.jcsr.2007.09.011.
Middleton, C.J. and Brownjohn, J.W.W. (2010), "Response of high frequency floors: A literature review", *Eng*. *Struct*., **32**, 337-352. https://doi.org/10.1016/j.engstruct.2009.11.003.
Mohammed, A.S., Pavicm A. and Racicm,V. (2018), "Improved model for human induced vibrations of high-frequency floors", *Eng*. *Struct*., **168**, 950-966. https://doi.org/10.1016/j.engstruct.2018.04.093.
NRCC 32349 (1990), *Building Vibration from Human Activities*, National Research Council Canada, Canada.
Osborne, K.P. and Ellis, B.R. (1990), "Vibration design and testing of a long-span lightweight floor", *Struct*. *Eng*., **68**, 81-186.
Pavic, P. and Reynolds, P. (2002), "Vibration serviceability of long-span concrete building floors: Part 1 - Review of background information", *Shock Vib*. *Digest*, **34**(3), 191-211.
Smith, I. and Chui, Y.H. (1988), "Design of lightweight wooden floors to avoid human discomfort", *Canadian J. Civil Eng*., **15**, 254-262. https://doi.org/10.1139/l88-033.
Williams, M.S. and Waldron, P. (1994), "Evaluation of methods for predicting occupant-induced vibrations in concrete floors", *Struct*. *Eng*., **72**, 334-340.
Willford, M., Young, P. and Field, C. (2007), "Predicting footfall-induced vibration: Part I", *Proceedings of the Institution of Civil Engineers*, *Structures & Buildings*, **160**(SB2), 65-72.

CC